

Stephen F. Austin State University
SFA ScholarWorks

Faculty Publications

Biology

2006

Heparin Modulates the 99-Loop of Factor IXa: EFFECTS ON REACTIVITY WITH ISOLATED KUNITZ-TYPE INHIBITOR DOMAINS


Pierre F. Neuenschwander
University of Texas Health Center at Tyler

Stephen R. Williamson
University of Texas Health Center at Tyler

Armen Nalian
Stephen F Austin State University

Kimberly J. Baker-Deadmond
University of Texas Health Center at Tyler

Follow this and additional works at: <https://scholarworks.sfasu.edu/biology>

 Part of the [Biochemistry Commons](#), [Enzymes and Coenzymes Commons](#), and the [Molecular Biology Commons](#)

Tell us how this article helped you.

Repository Citation

Neuenschwander, Pierre F.; Williamson, Stephen R.; Nalian, Armen; and Baker-Deadmond, Kimberly J., "Heparin Modulates the 99-Loop of Factor IXa: EFFECTS ON REACTIVITY WITH ISOLATED KUNITZ-TYPE INHIBITOR DOMAINS" (2006). *Faculty Publications*. 142.
<https://scholarworks.sfasu.edu/biology/142>

This Article is brought to you for free and open access by the Biology at SFA ScholarWorks. It has been accepted for inclusion in Faculty Publications by an authorized administrator of SFA ScholarWorks. For more information, please contact cdsscholarworks@sfasu.edu.

Heparin Modulates the 99-Loop of Factor IXa

EFFECTS ON REACTIVITY WITH ISOLATED KUNITZ-TYPE INHIBITOR DOMAINS*[§]

Received for publication, April 19, 2006, and in revised form, June 2, 2006. Published, JBC Papers in Press, June 9, 2006, DOI 10.1074/jbc.M603743200

Pierre F. Neuenschwander^{†1}, Stephen R. Williamson[‡], Armen Nalian[§], and Kimberly J. Baker-Deadmond[†]

From the [†]Department of Biochemistry, Biomedical Research Program, The University of Texas Health Science Center, Tyler, Texas 75708 and the [§]Department of Biotechnology, Stephen F. Austin State University, Nacogdoches, Texas 75962

Reactivity of factor IXa with basic pancreatic trypsin inhibitor is enhanced by low molecular weight heparin (enoxaparin). Previous studies by us have suggested that this effect involves allosteric modulation of factor IXa. We examined the reactivity of factor IXa with several isolated Kunitz-type inhibitor domains: basic pancreatic trypsin inhibitor, the Kunitz inhibitor domain of protease Nexin-2, and the first two inhibitor domains of tissue factor pathway inhibitor. We find that enhancement of factor IXa reactivity by enoxaparin is greatest for basic pancreatic trypsin inhibitor (>10-fold), followed by the second tissue factor pathway inhibitor domain (1.7-fold) and the Kunitz inhibitor domain of protease Nexin-2 (1.4-fold). Modeling studies of factor IXa with basic pancreatic trypsin inhibitor suggest that binding of this inhibitor is sterically hindered by the 99-loop of factor IXa, specifically residue Lys⁹⁸. Slow-binding kinetic studies support the formation of a weak initial enzyme-inhibitor complex between factor IXa and basic pancreatic trypsin inhibitor that is facilitated by enoxaparin binding. Mutation of Lys⁹⁸ to Ala in factor IXa results in enhanced reactivity with all inhibitors examined, whereas almost completely abrogating the enhancing effects of enoxaparin. The results implicate Lys⁹⁸ and the 99-loop of factor IXa in defining enzyme inhibitor specificity. More importantly, these results demonstrate the ability of factor IXa to be allosterically modulated by occupation of the heparin-binding exosite.

Factor IXa (fIXa)² is a vitamin K-dependent blood coagulation factor that is essential for the amplification or “consolidation” phase of blood coagulation (1, 2). As with other blood coagulation factors (namely factors VIIa, Xa, and thrombin) fIXa is a member of the serine protease family and shares a high

degree of homology with trypsin. Despite this homology, the blood coagulation enzymes differ drastically from trypsin in that their activities are profoundly modulated by the binding of various protein and non-protein cofactors. In the case of fIXa, the ability of activated factor VIII (fVIIIa), anionic phospholipid, and ionic calcium to enhance the procoagulant activity of fIXa is well documented (3–6); resulting in a 10⁹-fold increase in activity of fIXa. The molecular details of this conversion have not been defined in total and are the subject of intense investigation by numerous groups.

The major inhibitor of fIXa in plasma is antithrombin, whose reactivity with fIXa essentially requires heparin (7–9). Heparin is known to bind to antithrombin and sterically alter its conformation to allow this serpin to react with its target (10–13). Heparin also binds to fIXa (14) allowing long chains of heparin to additionally catalyze the interaction of fIXa with antithrombin via the formation of bridged complexes where heparin acts as a “template.” Recently, we have shown that low molecular weight heparin binding to fIXa enhances reactivity of fIXa with the Kunitz-type inhibitor BPTI (15), suggesting that oligosaccharide binding can also allosterically modulate the fIXa active site region. In this study we examine in greater detail the ability of heparin to modulate fIXa reactivity toward several isolated Kunitz-type inhibitor domains. We show that the modulatory effect of heparin can be completely abrogated by mutating a single amino acid residue in the 99-loop region of the extended fIXa active site cleft outside of the heparin binding exosite.

EXPERIMENTAL PROCEDURES

Materials—Factor IXa β , factor VIIa, factor XIa, and the factor X activator from Russell’s Viper venom were purchased from Hematologic Technologies Inc. (Essex Junction, VT). Recombinant soluble tissue factor (the extracellular domain of tissue factor) was expressed and purified from bacteria as previously described (16). Factor Xa was prepared from plasmas-derived factor X as previously described (17). Enoxaparin (Lovenox[®]) was purchased from Aventis Pharmaceuticals (Bridgewater, NJ). Purified heparin-derived oligosaccharides of 6, 10, 14, and 18 saccharide units (H6, H10, H14, and H18) were prepared and characterized essentially as described (18–20) and were a generous gift of Dr. Steven T. Olson, University of Illinois, Chicago, IL. Bovine serum albumin (Fraction V, fatty acid free) was from Calbiochem (La Jolla, CA), and ethylene glycol was from Fisher Scientific. The chromogenic substrate CBS 31.39 (CH₃SO₂-D-LGR-pNA) was purchased from Diagnostica Stago (Parsippany, NJ). All other reagents were of the highest quality available.

* This work was supported by National Institutes of Health Grant HL075696 (to P. F. N.). The costs of publication of this article were defrayed in part by the payment of page charges. This article must therefore be hereby marked “advertisement” in accordance with 18 U.S.C. Section 1734 solely to indicate this fact.

[§] The on-line version of this article (available at <http://www.jbc.org>) contains supplemental Table S1 and Figs. S1–S3.

¹ To whom correspondence should be addressed: Biomedical Research Lab C8, The University of Texas Health Science Center at Tyler, 11937 US Hwy. 271, Tyler, TX 75708. Tel.: 903-877-7678; Fax: 903-877-7679; E-mail: Pierre.Neuenschwander@uthct.edu.

² The abbreviations used are: fIXa, factor IXa; BPTI, basic pancreatic trypsin inhibitor; PN2-KPI, the isolated Kunitz-type inhibitor domain from protease nexin-2; TFPI, tissue factor pathway inhibitor; TFPI-K1, the isolated first Kunitz-type inhibitor domain of TFPI; TFPI-K2, the isolated second Kunitz-type inhibitor domain of TFPI; WT, wild-type; MES, 4-morpholineethanesulfonic acid; MOPS, 4-morpholinepropanesulfonic acid; Tricine, N-[2-hydroxy-1,1-bis(hydroxymethyl)ethyl]glycine.

Construction and Expression of Recombinant Inhibitors—Appropriate expression clones encoded for: BPTI (59 amino acids) (21, 22), PN2-KPI (61 amino acids corresponding to residues 285–344 of Protease Nexin-2) (23), TFPI-K1 (58 amino acids corresponding to residues 50–107 of TFPI) (24), and TFPI-K2 (59 amino acids corresponding to residues 121–178 of TFPI) (24). Each construct was directionally cloned into pET11a (Novagen) and verified by sequencing. Inhibitors were expressed as inclusion bodies in *Escherichia coli* strain BL21(DE3). Transformed bacterial cells were first grown to log phase at 37 °C in TB media containing 50 µg/ml carbenicillin. Protein expression was induced by addition of isopropyl 1-thio-β-D-galactopyranoside to 0.5 mM (0.1 mM for TFPI-K1) and the cells were allowed to continue growing for 4 h at 37 °C.

Inclusion bodies were isolated essentially as described (25) and solubilized with 6 M guanidine HCl containing 20 mM dithiothreitol, 50 mM Tris-HCl, pH 8.0, and 1 mM EDTA to obtain a total protein concentration of roughly 20 mg/ml. The solution was then clarified by centrifugation (16,000 × *g* for 30 min) and oxidative refolding (26) of each protein preparation was performed by rapid dilution into 20 volumes of buffer containing 50 mM Tris-HCl, pH 8.0, 1 M guanidine HCl, 1 mM EDTA, 2.5 mM oxidized glutathione (Sigma), and 1 mM dithiothreitol. The diluted protein solution was incubated at room temperature for 6 h with slow stirring for completion of protein refolding followed by exhaustive dialysis into an appropriate buffer for ion-exchange chromatography.

Construction and Expression of Wild-type and Mutant fIX—The coding sequence for wild-type fIX in pBR322 (27) was a generous gift of Dr. Earl Davie (University of Washington). The fIX coding sequence was removed into the mammalian expression vector pcDNA3 (Invitrogen) and sequenced to verify the correct orientation. This construct (pFN04) was used for expression of wild-type fIX as well as PCR-based mutagenesis (28) to generate fIXK98A essentially as previously described for constructing fVII mutants (29). Expression constructs were transfected into human 293 cells using Lipofectin® (Invitrogen) and high expressing clones isolated by limiting dilution.

Protein Purifications—Purification of refolded BPTI was accomplished by ion-exchange chromatography using Mono-S HR 5/5 (Amersham Biosciences) in 20 mM Tris-HCl, pH 8.0. The column was developed with a 0–1 M NaCl gradient and BPTI eluted as a single peak at roughly 0.43 M NaCl. The specific activity of recombinant BPTI preparations was equivalent to or better than that of commercial preparations of aprotinin (not shown). Purification of refolded PN2-KPI and TFPI-K2 was accomplished by ion-exchange chromatography using Mono-Q HR 5/5 (Amersham Biosciences) in 20 mM MES, pH 6.0. In both cases the column was developed with a 0–0.5 M NaCl gradient. PN2-KPI eluted at roughly 90 mM NaCl and TFPI-K2 eluted at roughly 50 mM NaCl. Purification of refolded TFPI-K1 was accomplished by affinity chromatography over a trypsin-agarose column. Trypsin-agarose was prepared by coupling 20 mg of L-1-tosylamido-2-phenylethyl chloromethyl ketone-treated trypsin (Worthington Biochemicals) to 2.5 ml of Affi-Gel 10 in 100 mM MOPS, pH 7.4, 10 mM CaCl₂, and 100 µg/ml leupeptin overnight at 4 °C. This was followed by blocking non-reacted sites with 1 M ethanolamine-HCl, pH 8.0.

Refolded TFPI-K1 was loaded onto the prepared trypsin-agarose column in 50 mM Tris-HCl, pH 7.5, 100 mM NaCl. The column was extensively washed with the same buffer before eluting the inhibitor with 10 mM HCl, pH 2.1, 100 mM NaCl. The pH of the eluted fractions was immediately neutralized with 0.02 volumes of 2 M Tris buffer. All inhibitors were judged >95% pure by SDS-PAGE.

Recombinant human wild-type fIX and fIXK98A were isolated from 293 cell supernatants using a combination of ion-exchange and heparin affinity chromatography. A 10-fold concentrate of cell supernatant was diluted 2-fold with deionized water to reduce the ionic strength before loading a 150-ml DEAE FF Sepharose (Amersham Biosciences) column equilibrated in 25 mM sodium citrate, pH 6.0, 33 mM NaCl, and 1 mM benzamidine. After loading, the column was extensively washed in the same buffer before elution of the fIX protein with a 0.033–0.4 M NaCl gradient over 10 column volumes. The fIX protein peak was identified by clotting activity, pooled, and dialyzed *versus* 50 mM Tris-HCl, pH 7.5, 100 mM NaCl before heparin affinity chromatography using either POROS® HE2 (Applied Biosystems) or HiPrep™ Heparin FF 16/10 (Amersham Biosciences) and eluting with a NaCl gradient. Wild-type fIX and fIXK98A both eluted as single peaks at roughly 0.46 M NaCl.

Wild-type and mutant fIX proteins were activated with the purified factor X activator from the venom of Russell's viper, which also cleaves fIX after Arg¹⁸⁰ to generate active enzyme (fIXα). The activated enzyme was purified away from the venom protease by subsequent heparin affinity chromatography essentially as described above using HiTrap™ Heparin HP (Amersham Biosciences). Although the activation peptide remains attached to the light chain of fIXα, this enzyme retains 100% amidolytic activity compared with fIXαβ (activation peptide proteolytically removed) and is comparable with fIXαβ in kinetics of inhibition by Kunitz-type inhibitors (see "Results"). Unless indicated otherwise, the fIXα form was used in experiments.

Clotting Assays—Coagulant activities of wild-type and mutant fIXa proteins were assayed by a standard single-stage clotting assay using a Coag-a-mate XM (Organon Teknica) coagulometer, fIX-deficient plasma (George King Biomedical), and APTT Reagent (Sigma).

Reactive Site Titration of Inhibitors—The active concentration of inhibitor preparations was determined by reactive site titration essentially as described (23) using 10 nM active site-titrated trypsin (30) and S-2222 substrate (Chromogenix, Milano, Italy) to measure residual trypsin activity after a 15-min incubation period. This method assumes a 1:1 stoichiometry of inhibitor and trypsin. Amino acid analysis performed on an initial PN2-KPI preparation indicated an equivalent concentration as that determined by reactive site titration (not shown).

Active Site Titration of fIXa Enzymes—Active concentrations of wild-type and mutant fIXa preparations were determined by active site titration using biotin-EGR-ck (Hematologic Technologies Inc.) essentially as described (31). Briefly, wild-type or mutant fIXa (roughly 5 µM) were incubated with 150 µM biotin-EGR-ck in 50 mM Tricine, pH 8.0, 200 mM NaCl, 10 mM CaCl₂,

Modulation of the fIXa 99-Loop by Heparin

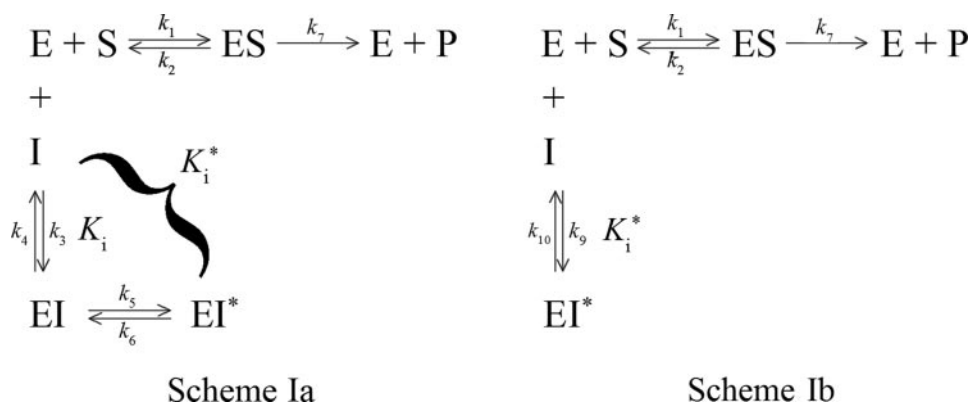


FIGURE 1. Reversible slow-binding enzyme inhibition schemes. Schemes Ia and Ib both describe the reversible slow-binding inhibition of an enzyme (E) by an inhibitor (I) resulting in competitive inhibition of substrate (S) binding and the subsequent reduction in product (P) formation (33, 34). Both schemes show the formation of the Michaelis complex (ES) as described classically by k_1 , k_2 , and k_7 . In Scheme Ia inhibition of enzyme occurs in two distinct steps: 1) formation of a loose EI inhibitory complex described by k_3 and k_4 , where $k_4/k_3 = K_i$; 2) Isomerization of EI to EI^* described by k_5 and k_6 . In Scheme Ib the binding of inhibitor and isomerization of the complex are simultaneous and not distinguishable. In this case k_9 and k_{10} represent the overall on- and off-rate constants. This situation can arise when k_4 and k_3 are very slow (rate-limiting) compared with k_5 and k_6 . In both schemes the overall inhibition is described by K_i^* , which is the final inhibition constant observed at equilibrium of the system.

and 30% ethylene glycol for 24 h at room temperature. Biotin-EGR-fIXa was then quantified by enzyme-linked immunosorbent assay using a goat anti-fIX polyclonal capture antibody and alkaline phosphatase-conjugated streptavidin. These were compared with a standard line made using native fIXa β to determine active concentrations for all fIXa enzyme preparations.

Equilibrium Enzyme Inhibition Assays—Reversible competitive inhibition of fIXa amidolytic activity at equilibrium was measured at 25 °C using final concentrations of 25 nM fIXa, 5 mM CaCl₂ and the indicated concentrations of enoxaparin and inhibitor in the presence of 30% ethylene glycol as previously described (15). The addition of ethylene glycol enhances the enzymatic activity of fIXa toward CBS 31.39 roughly 20-fold (32). Previous studies by us as well as control experiments performed with each inhibitor examined showed that the inclusion of ethylene glycol in the assay has no effect on the reactivity of fIXa with these inhibitors (15). Values of the final equilibrium inhibition constant ($K_{i,eq}$) were estimated as described (15, 29) using Equation 1. This equation describes simple reversible competitive inhibition where v_o is the steady state rate obtained in the absence of inhibitor, v_s is the steady state rate at each concentration of inhibitor, S is the experimental substrate concentration, and K_m is the Michaelis constant for substrate hydrolysis.

$$v_s = v_o \frac{K_{i,eq}(1 + S/K_m)}{K_{i,eq}(1 + S/K_m) + S} \quad (\text{Eq. 1})$$

Slow-binding Enzyme Inhibition Analysis—Kinetic parameters for slow-binding inhibition were obtained using Equations 2–5 as derived by others (33, 34) and are described in Schemes Ia and Ib (Fig. 1). In both of these schemes the non-covalent enzyme-inhibitor complex, EI , isomerizes into EI^* ; either after significant formation of the EI complex (Scheme Ia) or without significant accumulation of the EI complex (Scheme Ib). In both cases, the overall inhibition constant describing genera-

tion of EI^* is defined as K_i^* , which is equivalent to $K_{i,eq}$ obtained from equilibrium experiments (above). In cases following Scheme Ia, the parameter K_i^* can be further broken down to obtain K_i , which describes the establishment of the initial “loose” EI complex, k_5 and k_6 (see below).

Final reaction conditions were the same as described above for equilibrium studies. In these assays, however, the fIXa was preincubated with or without enoxaparin for 15 min at 25 °C in the reaction mixture before the combined addition of inhibitor and substrate at time 0. The absorbance at 405 nm was then monitored for up to 30 min in a ThermoMax microplate reader (Molecular Devices) set at 25 °C to monitor substrate hydrolysis using

KINEMAX software (written and kindly provided by Dr. Jolyon Jesty, SUSB, Stony Brook, NY). Data for each generated curve were fitted with the following integrated rate equation describing slow-binding inhibition,

$$A = v_s t + (v_o - v_s)(1 - e^{-k_{obs}t})/k_{obs} + A_o \quad (\text{Eq. 2})$$

where A is the absorbance at 405 nm at any time, t . Fits of progress curves with Equation 2 yield values for A_o (the initial absorbance at $t = 0$), v_o (the initial rate of substrate hydrolysis), v_s (the steady-state rate of substrate hydrolysis), and k_{obs} (the apparent first-order rate constant for inhibition).

For analyses using Scheme Ia, values of k_6 (the reverse rate constant for EI^* isomerization) were determined from progress curves above using the following relationship.

$$k_6 \text{ or } k_{10} = k_{obs}v_s/v_o \quad (\text{Eq. 3})$$

Values of k_5 and initial K_i (defined as k_4/k_3) were then obtained from secondary plots of k_{obs} versus I using the following hyperbolic equation.

$$k_{obs} = k_6 + k_5I/(1 + K_i(1 + S/K_m)) \quad (\text{Eq. 4})$$

For analyses using Scheme Ib, values of k_{10} were obtained from progress curves also using Equation 3. However, in these cases v_o does not vary with inhibitor concentration and a plot of k_{obs} versus I yields a straight line, indicating conditions where $K_i(1 + S/K_m) \gg I$. Thus for Scheme Ib EI formation is insignificant and EI^* can be considered formed directly from $E + I$. For these cases the following linear equation is applicable for obtaining an estimate of k_9 , the apparent second-order on-rate constant,

$$k_{obs} = k_{10} + k_9I/(1 + S/K_m) \quad (\text{Eq. 5})$$

where the y intercept reflects k_{10} and the slope of the line is equal to $k_9/(1 + S/K_m)$. Alternatively, k_9 can be obtained from K_i^* , which is equivalent to $K_{i,eq}$ in Equation 1, using the relationship $k_9 = k_{10}/K_i^*$.

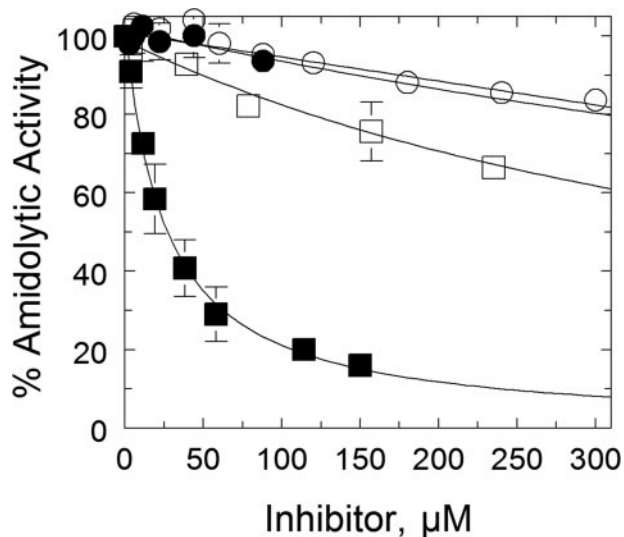


FIGURE 2. **Inhibition of fIXa β by isolated Kunitz-type inhibitor domains.** fIXa β (25 nM) was titrated with the indicated concentrations of BPTI (\circ), TFPI-K1 (\bullet), TFPI-K2 (\square), and PN2-KPI (\blacksquare). The remaining fIXa amidolytic activity at equilibrium was then measured and values were normalized to the activity of fIXa in the absence of inhibitor (100%). Data were fitted with Equation 1 (lines) to obtain values of $K_{i,eq}$ (see text).

Although fits with Equations 4 or 5 yield estimates of k_6 or k_{10} , respectively, the values reported herein were obtained from Equation 3 using the more accurate fits of progress curves to Equation 2 and then verified in fits with Equations 4 or 5. Experimental values of S as well as experimentally determined values of K_m (defined in the traditional manner as $(k_2 + k_7)/k_1$ in Schemes Ia and Ib) were used as necessary in all fitting procedures. All regression procedures were performed using Slide-WritePlus 6.0 (Advanced Graphics Software), which uses the Levenberg-Marquardt algorithm.

RESULTS

Previous studies (15) by us have shown that whereas fIXa is resistant to inhibition by the Kunitz-type inhibitor BPTI, this resistance is somewhat alleviated by enoxaparin, leading to a roughly 10-fold enhancement in the equilibrium inhibition constant. To gain further insight into mechanisms of fIXa selectivity and its modulation by heparin we undertook an examination of the reactivity of fIXa with several isolated Kunitz-type inhibitor domains: BPTI, PN2-KPI, TFPI-K1, and TFPI-K2. Each of these inhibitors was expressed in *E. coli* using standard recombinant techniques, purified to homogeneity and quantified by reactive site titration as described under "Experimental Procedures." The isolated PN2-KPI inhibitor domain was found to react with high affinity toward factor XIa, yielding a $K_{i,eq}$ of roughly 400 pM (see supplemental data). Similarly, preliminary studies indicated that preparations of isolated TFPI-K1 domain inhibited the complex of factor VIIa and soluble tissue factor with high affinity ($K_{i,eq} = 400$ nM) and weakly inhibited factor Xa ($K_{i,eq} > 1.5$ μ M). Conversely, the isolated TFPI-K2 domain inhibited factor Xa with high affinity ($K_{i,eq} = 24$ nM) and the factor VIIa-tissue factor complex with reduced affinity ($K_{i,eq} = 7$ μ M). These results are consistent with the expected reactivity of the isolated inhibitor domains (35, 36)

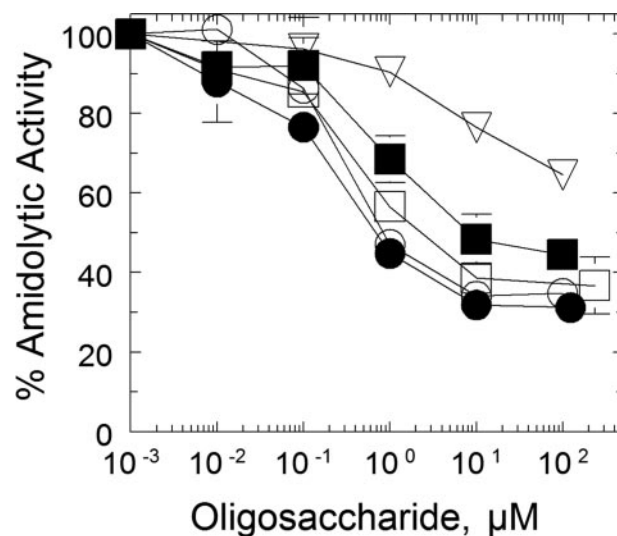


FIGURE 3. **Support of BPTI inhibition of fIXa by short chain oligosaccharides.** The ability of heparin oligosaccharides with progressively shorter chain lengths to support enhancement of fIXa reactivity with BPTI was examined using 25 nM fIXa β , 308 μ M BPTI, and the indicated concentrations of heparin-derived oligosaccharides (18–20) from 0.01 to 200 μ M. Saccharide chain lengths were H18 (\bullet), H14 (\square), H10 (\blacksquare), and H6 (∇). Enoxaparin (H15) is shown for comparison (\circ). The fIXa activities were normalized to the activity of fIXa in the absence of added oligosaccharide.

and demonstrate the correct folding and inhibitor activity of the inhibitors examined.

The abilities of these isolated Kunitz inhibitor domains to inhibit fIXa β are compared in Fig. 2. As expected, fIXa exhibited remarkable specificity toward these inhibitors despite their high homology. Of the inhibitors examined, PN2-KPI showed the highest level of reactivity ($K_{i,eq} = 10$ μ M), followed by TFPI-K2 ($K_{i,eq} = 336$ μ M), BPTI ($K_{i,eq} > 500$ μ M), and TFPI-K1 ($K_{i,eq} > 1$ mM). Consistent with our previous observations, enoxaparin was able to enhance the reactivity of fIXa with BPTI more than 10-fold ($K_{i,eq} = 46$ μ M). Surprisingly, however, this same level of enhancement by enoxaparin was not observed with any of the other inhibitors examined; TFPI-K2 and PN2-KPI each showed only a small, but consistent, enhancement in reactivity with enoxaparin (1.7- and 1.4-fold, respectively; $K_{i,eq}$ values of 203 and 7 μ M) and TFPI-K1 showed no measurable enhancement in reactivity with enoxaparin.

The highly basic nature of BPTI compared with the other isolated Kunitz domains along with its ability to bind to heparin (albeit weakly; $K_d = 172$ μ M (15)) raised the potential that enoxaparin, although short (15 saccharide units; H15), may retain some capacity to facilitate the interaction of BPTI with fIXa via a bridging-type mechanism. Although unlikely based on previous equilibrium kinetic studies and the level of enoxaparin used in these experiments (10 μ M; or $0.06 \times K_d$ for BPTI binding versus $78 \times K_d$ for fIXa binding), this issue was examined by using increasing concentrations of enoxaparin as well as progressively smaller heparin oligosaccharides; H18, H14, H10, and H6 (18–20). As shown in Fig. 3, the typical bell-shaped profile for bridging-type mechanisms was not observed at enoxaparin concentrations ranging from 1 nM to >100 μ M. In addition, and of greater significance, is the observation that progressively smaller oligosaccharides do not lose the ability to enhance reactivity of fIXa. These results along with previous

Modulation of the fIXa 99-Loop by Heparin

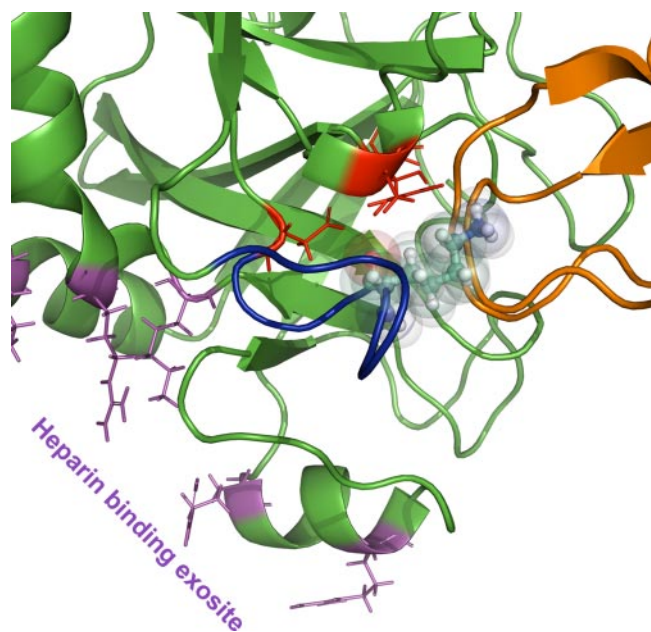


FIGURE 4. **Hypothetical model of the inhibited fIXa-BPTI complex.** A hypothetical fIXa-BPTI complex model was constructed using Discovery Studio software (Accelrys) based on known crystal structures of fIXa (PDB code 1RFN) and fVIIa-BPTI_{5L15} (PDB code 1FAK) using molecular replacement. The structure revealed potential steric hindrance between BPTI and the 99-loop of fIXa, specifically Lys⁹⁸ (central ball and stick structure with van der Waals radii). BPTI is depicted in orange; fIXa is depicted in green with the 99-loop in blue; the heparin binding exosite residues in fIXa (14) are depicted as violet sticks; and the fIXa active site triad residues (Ser¹⁹⁵, His⁵⁷, and Asp¹⁰²) are depicted as red sticks.

kinetic studies support the ability of heparin to modulate fIXa reactivity via a mechanism other than bridging, and are consistent with allosteric modulation of the fIXa protease domain.

To gain further insight into the potential mechanism of heparin modulation of fIXa, we prepared a rudimentary hypothetical model of the fIXa-BPTI complex using available crystal structures of BPTI (37), fIXa (38), and the fVIIa-BPTI_{5L15} complex (39). Using the latter structure as a template, superimposition of the native BPTI structure over the mutant BPTI structure along with superimposition of the fIXa structure over the fVIIa structure (Discovery Studio v 1.1; Accelrys Inc.) suggested a constriction of the fIXa active site in a manner that may be expected not to readily accommodate BPTI. The main site of steric hindrance seemed to be with the 99-loop of fIXa, specifically residue Lys⁹⁸ (Fig. 4). We hypothesized that heparin binding may act to allosterically modulate the 99-loop of fIXa.

Based on this hypothesis, we examined a mutant of fIXa in which Lys⁹⁸ was mutated to Ala (fIXK98A). Wild-type and mutant forms of fIXa were expressed in human 293 cells and purified to >95% homogeneity as judged by SDS-PAGE (Fig. 5A). The fIXK98A mutant was found to retain 100% clotting activity compared with wild-type fIXa (Fig. 5B) and upon activation retained near normal amidolytic activity toward CBS 31.39 substrate (Table 1).

We first examined the kinetics of inhibition of WT fIXa by BPTI using the slow-binding inhibition model (33, 34). In this model (Fig. 1, Scheme 1a) BPTI forms an initial loose inhibitory complex with fIXa (defined by K_i and the rate constants k_3 and k_4) followed by the slow isomerization of the EI com-

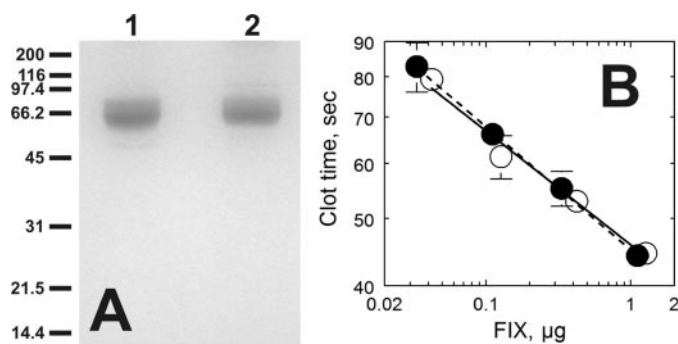


FIGURE 5. **A**, SDS-PAGE analysis of recombinant WT fIX and fIXK98A. Five μg of purified WT fIX (lane 1) and fIXK98A (lane 2) were loaded onto a 12% polyacrylamide gel under reducing conditions for SDS-PAGE. The resulting gel was stained with Coomassie Brilliant Blue G-250. Molecular weight markers are indicated on the left. **B**, clotting activity of fIXK98A versus WT fIX. Standard single-stage clotting assays were performed on recombinant WT fIX (○) and fIXK98A (●), which showed equivalent coagulant activity.

TABLE 1
Kinetic parameters for CBS 31.39 hydrolysis by WT fIXa versus fIXaK98A

Obtained by fitting the data with the Michaelis-Menton equation. Values shown are \pm S.E., $n = 6$.

Enzyme	K_m	k_{cat}	k_{cat}/K_m
	M	s^{-1}	$M^{-1} s^{-1}$
WT fIXa	$3.78 (\pm 0.08) \times 10^{-3}$	$16.5 (\pm 0.69)$	$4.37 (\pm 0.08) \times 10^3$
fIXaK98A	$1.58 (\pm 0.02) \times 10^{-3}$	$6.23 (\pm 0.43)$	$3.98 (\pm 0.27) \times 10^3$

plex to EI^* (defined by the rate constants k_5 and k_6). This results in overall inhibition of the enzyme as defined by K_i^* , which is equivalent to the $K_{i,eq}$ value determined in equilibrium experiments. The progress curves obtained for BPTI inhibition of WT fIXa in the absence and presence of a saturating level of enoxaparin are shown in Fig. 6, A and B, respectively. The shapes of the progress curves support the slow binding nature of BPTI with recombinant WT fIXa. These curves were identical to control reactions performed with fIXa β (not shown) and are well described by Equation 2. Values of k_6 subsequently obtained using Equation 3 showed no significant differences in the absence or presence of enoxaparin; $k_6 = 2.7 (\pm 1.5) \times 10^{-3} s^{-1}$ without enoxaparin and $1.2 (\pm 0.2) \times 10^{-3} s^{-1}$ with enoxaparin.

As an independent verification of k_6 an experiment was performed where $5 \mu\text{M}$ fIXa was incubated with $231 \mu\text{M}$ BPTI in the presence of enoxaparin for 20 min, followed by a rapid 1,000-fold dilution into the same buffer also containing enoxaparin. Timed aliquots of this diluted mixture were removed into 1 mM CBS 31.39 substrate to monitor the recovery of enzyme activity over time (Fig. 6B, inset). Under these conditions, the BPTI concentration is over 200-fold lower than the apparent $K_{i,eq}$ and thus k_6 can be approximated by the rate constant describing recovery of activity (33, 34). Fitting the data with a single exponential equation yielded a value for this rate constant that reasonably supports the value of k_6 obtained above ($1.9 \times 10^{-3} s^{-1}$).

From fits of the progress curves in Fig. 6, A and B, with Equation 2, secondary plots of k_{obs} versus BPTI for WT fIXa show little or no curvature (Fig. 6C). This suggests a very high initial K_i value and an indeterminate value for k_5 . These observations as well as the lack of change in v_o with increasing inhibitor

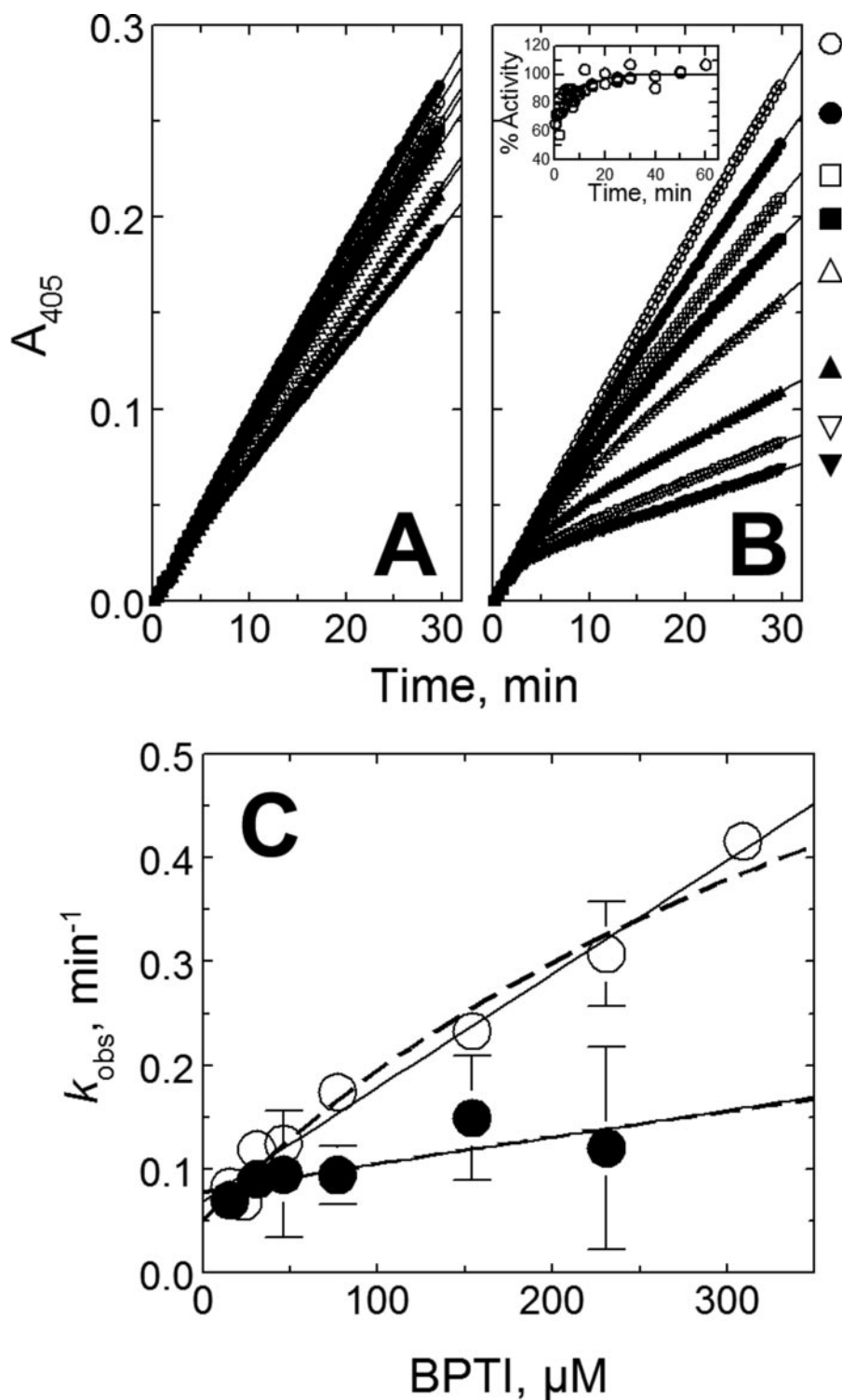


FIGURE 6. **Slow-binding inhibition of WT fIXa by BPTI.** *A*, progress curves of WT fIXa inhibition by BPTI in the absence of enoxaparin. *B*, progress curves of WT fIXa inhibition by BPTI in the presence of 10 μM enoxaparin. BPTI concentrations used were: 0 (\circ), 15.4 (\bullet), 30.8 (\square), 46.2 (\blacksquare), 77 (\triangle), 154 (\blacktriangle), 231 (∇), and 308 μM (\blacktriangledown). *Inset*, recovery of enzymatic activity of WT fIXa after inhibition with BPTI and enoxaparin. The inhibited fIXa-BPTI complex was diluted 1,000-fold and timed aliquots were removed into CBS 31.39 substrate to measure recovery of enzymatic activity over time. The activities were compared with a parallel reaction done in the absence of inhibitor to normalize values to 100%. The data were fitted with a single-exponential equation to determine a value for k (roughly equivalent to k_{10} , see text). *C*, secondary plots of k_{obs} from panels *A* and *B* versus BPTI concentration for WT fIXa in the absence (\bullet) and presence (\circ) of enoxaparin. Data were fitted with Equation 5 (solid lines). Kinetic constants obtained are given in Table 2. Refitting of the data using Equation 4 as described under "Discussion" is also shown (dashed lines).

concentrations (*cf.* Fig. 6, *A* and *B*) are diagnostic for Scheme Ib. The data of Fig. 6C were thus fitted with Equation 5 to obtain estimates for the apparent second-order rate constant; $k_6 = 5.4 \text{ M}^{-1} \text{ s}^{-1}$ without enoxaparin and $23 \text{ M}^{-1} \text{ s}^{-1}$ with enoxaparin. The value obtained above for k_6 (k_{10} in Scheme Ib) is consistent with the values obtained for k_{10} using Equation 5; $k_{10} = 1.3 \times 10^{-3} \text{ s}^{-1}$ without enoxaparin and $1.2 \times 10^{-3} \text{ s}^{-1}$ with enoxaparin.

A similar slow-binding kinetic analysis was performed with WT fIXa and PN2-KPI. In contrast to what was observed with BPTI, secondary plots of k_{obs} versus PN2-KPI were hyperbolic (not shown) and well described by Scheme Ia, yielding the values of K_i , k_5 , and k_6 given in Table 2. The role of Lys⁹⁸ and the 99-loop of fIXa in inhibition of fIXa by both BPTI and PN2-KPI were next examined using fIXaK98A. This mutant fIXa showed increased reactivity toward all of the inhibitors examined (Table 3). More importantly, the enhancing effect of enoxaparin was substantially reduced when compared with WT fIXa. Detailed analysis of the slow-binding kinetics of inhibition of fIXaK98A by BPTI revealed that the major difference compared with WT fIXa was the enhanced formation of the initial enzyme-inhibitor complex, as seen visually by the variation in initial rate (v_0) of progress curves (Fig. 7, *A* and *B*) and the hyperbolic nature of secondary plots (Fig. 7C). Although enoxaparin significantly enhanced the reactivity of both WT fIXa and fIXaK98A toward BPTI (Table 2), the effect on the mutant was much reduced and was completely abrogated for its inhibition by PN2-KPI.

DISCUSSION

Previous studies by us have demonstrated that heparin binding to fIXa enhances fIXa reactivity with BPTI (15). Whereas in that study unfractionated heparin was found to have a slightly greater effect, enoxaparin retained most of the ability to enhance fIXa reactivity.

Modulation of the fIXa 99-Loop by Heparin

TABLE 2

Kinetic constants for inhibition of fIXa and fIXaK98A by BPTI and PN2-KPI

Unless indicated otherwise, values of kinetic constants were obtained using Equations 3 and 4 (see text).

Enzyme	Inhibitor	Enoxaparin	K_i <i>M</i>	k_5 <i>s⁻¹</i>	k_6 <i>M⁻¹ s⁻¹</i>	k_6 or k_{10}^a <i>s⁻¹</i>	$K_i^* \text{ calc}^b$ <i>M</i>
WT fIXa	BPTI	–	$2.1 \times 10^{-3} \text{ c}$		5.4	$2.67 (\pm 1.50) \times 10^{-3}$	
		+	$4.1 \times 10^{-4} \text{ c}$		23	$1.17 (\pm 0.17) \times 10^{-3}$	
fIXaK98A	PN2-KPI	–	2.0×10^{-5}	1.3×10^{-2}		$3.67 (\pm 2.66) \times 10^{-3}$	4.4×10^{-6}
		+	3.3×10^{-5}	1.3×10^{-2}		$3.50 (\pm 0.67) \times 10^{-3}$	7.0×10^{-6}
	BPTI	–	1.3×10^{-4}	1.5×10^{-2}		$2.33 (\pm 0.67) \times 10^{-3}$	1.7×10^{-5}
		+	8.8×10^{-5}	1.6×10^{-2}		$1.65 (\pm 0.33) \times 10^{-3}$	8.2×10^{-6}
PN2-KPI	–	6.8×10^{-6}	1.4×10^{-2}		$2.33 (\pm 1.00) \times 10^{-3}$	9.7×10^{-7}	
	+	8.0×10^{-6}	1.4×10^{-2}		$2.00 (\pm 0.83) \times 10^{-3}$	1.0×10^{-6}	

^a Values are k_{10} for WT fIXa with BPTI (Scheme 1b) and k_6 for others (Scheme 1a) \pm S.D. ($n \geq 7$).

^b Calculated from k_5 , k_6 , and K_i using the relationship $K_i^* = k_6 K_i / (k_5 + k_6)$ (33, 34).

^c Determined from refits of the data in Fig. 6C with Equation 4 using k_5 obtained for fIXaK98A and BPTI (see "Discussion").

TABLE 3

Equilibrium inhibition constants for Kunitz-type inhibitors and WT fIXa versus fIXaK98A

Enzyme	Enoxaparin	$K_{i,eq}$ <i>M</i>			
		BPTI	TFPI-K1	TFPI-K2	PN2-KPI
WT fIXa	–	$6.46 (\pm 0.83) \times 10^{-4}$	$>1.0 \times 10^{-3}$	$4.14 (\pm 0.51) \times 10^{-4}$	$9.52 (\pm 1.0) \times 10^{-6}$
	+	$5.91 (\pm 0.32) \times 10^{-5}$	$>1.0 \times 10^{-3}$	$2.57 (\pm 0.71) \times 10^{-4}$	$6.84 (\pm 0.76) \times 10^{-6}$
fIXaK98A	–	$2.48 (\pm 0.54) \times 10^{-5}$	$1.31 (\pm 0.23) \times 10^{-4}$	$4.36 (\pm 0.51) \times 10^{-5}$	$1.31 (\pm 0.17) \times 10^{-6}$
	+	$1.32 (\pm 0.24) \times 10^{-5}$	$1.11 (\pm 0.42) \times 10^{-4}$	$2.83 (\pm 0.11) \times 10^{-5}$	$1.19 (\pm 0.19) \times 10^{-6}$

The conclusion that heparin can modulate the active site of fIXa is supported in the present study by several observations, not the least of which is the ability of short chain oligosaccharides to retain the ability to enhance fIXa reactivity with BPTI. Whereas the shortest oligosaccharide examined (H6) requires higher concentrations than do H10–H18, the higher IC₅₀ for H6 is consistent with the reduced binding energy one may expect for a small oligosaccharide whose projected length would contact only two thirds of the heparin binding exosite: based on available crystal structures (Protein Data Bank codes 1E0O and 1BFC) the length of a decasaccharide is expected to be ~38 Å and that of a hexasaccharide is expected to be ~23 Å at full extension. This is compared with the measured length of the identified heparin binding site on fIXa (~35 Å) based on mutational studies (14).

With respect to the inhibition of fIXa by BPTI, two main conclusions may be drawn from these studies: 1) fIXa residue Lys⁹⁸ is in part responsible for protecting fIXa from inhibition by BPTI, likely via steric hindrance. Removal of this steric obstruction by mutation of Lys⁹⁸ results in greater inhibition of fIXa by BPTI (26-fold enhancement). 2) Heparin binding to fIXa in part counteracts the steric protection provided by Lys⁹⁸. Mutation of Lys⁹⁸ results in a reduction in the ability of heparin to further enhance reactivity of fIXa with BPTI (roughly 2-fold effect for fIXaK98A compared with >10-fold effect with WT fIXa). The lack of complete abrogation of the effect of heparin suggests that other as yet undefined factors also play a role in BPTI inhibition of fIXa and its response to heparin. This is likely due to the movement of more than simply Lys⁹⁸ and may or may not involve other residues in the 99-loop or even the entire loop.

It is important to note that the reduction in the effect of heparin with the fIXaK98A mutant is not merely due to reduced heparin binding because fIXaK98A retained the ability to bind to heparin-Sepharose and eluted at the same salt con-

centration as WT fIXa during purification procedures. In support of this, preliminary experiments performed by titrating fIXaK98A with enoxaparin in the presence of 100 μM BPTI yielded results consistent with the high nanomolar affinity for enoxaparin previously observed with fIXaβ ($K_d = 128$ nM (15)). No further increase in inhibition of fIXaK98A by BPTI was observed when the enoxaparin level was increased from 1 to 10 μM (not shown). Because all experiments were conducted using 10 μM enoxaparin, it seems reasonable to assume that fIXaK98A was saturated in these experiments.

Whereas the data for fIXa with BPTI in Fig. 6C are consistent with Scheme 1b, this scheme is essentially a simplified version of Scheme 1a with a very large value for K_i (33, 34). Examination of the Scheme 1a kinetic constants in Table 3 for fIXa with PN2-KPI as well as those for fIXaK98A with both inhibitors shows fairly consistent values for k_5 and k_6 . This suggests that once formed, isomerization of the EI complex to EI* is essentially the same for any of the enzyme-inhibitor pairs examined. Based on this it seems reasonable to tentatively extend the value of k_5 to the WT fIXa-BPTI pair and re-examine the data of Fig. 6C with respect to Scheme 1a. This results in fits to Equation 4 shown in Fig. 6C as *dashed lines* and yields initial K_i values of 2.1×10^{-3} M and 4.1×10^{-4} M in the absence and presence of enoxaparin, respectively. This 5-fold difference in K_i along with ~2-fold difference in k_6 (k_{10}) for this enzyme-inhibitor pair (Table 2) would seem to account for the ~10-fold effect of enoxaparin observed in $K_{i,eq}$ (Table 3). Unfortunately, the rather large errors in the values of k_6 (k_{10}) preclude definitive conclusions concerning potential effects of enoxaparin on this rate constant.

Regardless, these results are consistent with a very weak initial interaction of fIXa with BPTI. Enoxaparin binding to the heparin binding exosite in fIXa at least in part acts to allosterically modulate the 99-loop of fIXa in a manner that facilitates this initial interaction. The results with BPTI are in contrast to

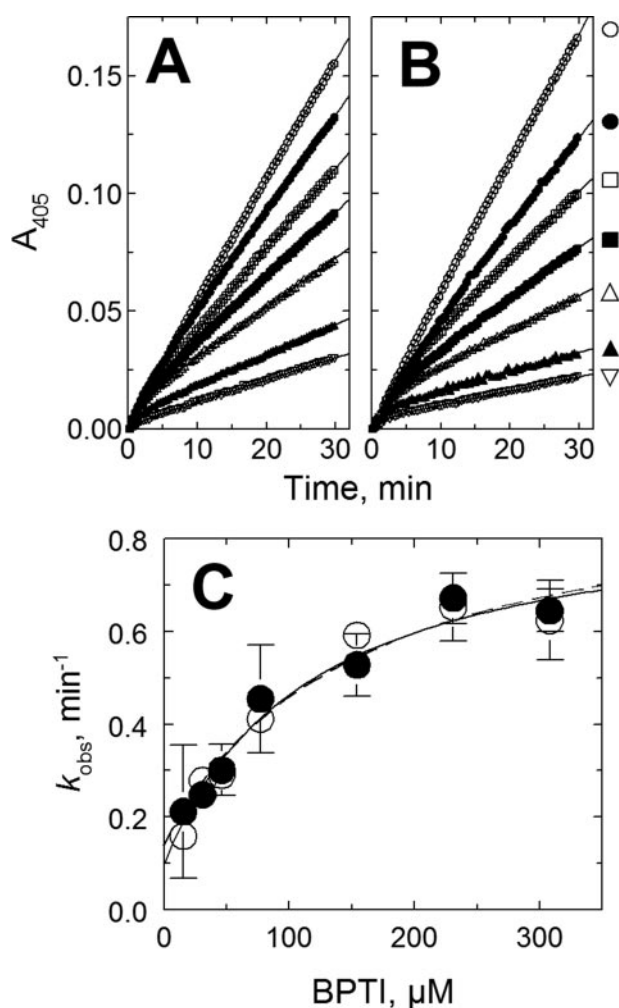


FIGURE 7. **Slow-binding inhibition of fIXaK98A by BPTI.** *A*, progress curves of fIXaK98A inhibition by BPTI in the absence of enoxaparin. *B*, progress curves of fIXaK98A inhibition by BPTI in the presence of 10 μM enoxaparin. BPTI concentrations used were: 0 (\circ), 15.4 (\bullet), 30.8 (\square), 46.2 (\blacksquare), 77 (\triangle), 154 (\blacktriangle), and 231 μM (∇). *C*, secondary plots of k_{obs} from panels *A* and *B* versus BPTI concentration for fIXaK98A in the absence (\bullet) and presence (\circ) of enoxaparin. Data were fitted with Equation 4 (lines). Kinetic constants obtained are given in Table 2.

the interaction of fIXa with TFPI-K1, TFPI-K2, or PN2-KPI. The former shows no effect of heparin binding, whereas the latter two show only small (but reproducible) responses to heparin binding. These results would suggest that these three Kunitz inhibitor domains are not as greatly hindered as BPTI by the 99-loop of fIXa. Indeed, mutation of Lys⁹⁸ enhanced the inhibition by TFPI-K1 roughly 8-fold, TFPI-K2 roughly 9-fold, and by PN2-KPI only 6–7-fold. Interestingly, however, the effect of enoxaparin on fIXaK98A reactivity toward both TFPI-K1 and TFPI-K2 was unchanged, whereas that for PN2-KPI was completely abrogated. Thus, there is some disparity in the role of Lys⁹⁸ and additional effects of heparin binding are likely.

Previous studies have demonstrated the ability of full-length TFPI to inhibit fIXa with an affinity of roughly 300 nM (40). It is thus interesting that neither the isolated TFPI-K1 nor isolated TFPI-K2 domains retain very high reactivity with fIXa. Preliminary studies indicated that our preparations of isolated inhibitor domains were of good quality and activity. This would seem to indicate that the folding and activity of these inhibitor

domains are correct. Taken as a whole, the results here would seem to imply that either the connecting regions of TFPI are important for its activity toward fIXa or other structural/topological elements are involved. Nonetheless, it is likely that the TFPI-K2 domain is the inhibitor domain of TFPI most likely responsible for interaction with fIXa. Although the isolated third Kunitz repeat of TFPI was not examined in this study, this domain is likely not an active inhibitor domain *per se* (41).

The ability of heparin to allosterically modulate the active site of fIXa demonstrates the ability of fIXa to respond to binding at this exosite. This observation is made more interesting by the observation by Sheehan *et al.* (42, 43) that the heparin binding exosite in part represents a fVIIIa interactive site on fIXa. Thus, whereas heparin binding in itself may inhibit fIXa coagulant activity via steric hindrance of fVIIIa binding, fVIIIa binding to this exosite may inversely act to allosterically modulate fIXa in an as yet undefined manner. Although previous studies found no effect of fVIIIa on fIXa inhibition by the isolated PN2-KPI domain (44), this is consistent with our observations here using enoxaparin in place of fVIIIa and does not preclude potential effects of fVIIIa toward other inhibitors. It thus remains possible that occupation of this exosite by fVIIIa, like heparin, results in inhibitor-specific modulatory effects. Alternatively, the modulating effect of heparin on the 99-loop may be simply due to heparin-specific electrostatic forces that are introduced by heparin binding in close proximity to Lys⁹⁸ (*cf.* Fig. 4). These forces may or may not be mimicked by fVIIIa binding. Further clarification of these issues must await future studies.

The allosteric modulation of fIXa by enoxaparin is somewhat reminiscent of the effect of thrombomodulin on the interaction of thrombin with BPTI, where binding of thrombomodulin alters the conformation of one of the specificity loops (60-loop) at the mouth of the active site of thrombin, resulting in enhanced reactivity with BPTI (45). Interestingly, in that study the chondroitin sulfate moiety of thrombomodulin (which binds to the heparin binding site on thrombin; anion binding exosite 2) further enhanced the inhibition of an E192Q mutant of thrombin but not wild-type thrombin. Comparison of the sequence of fIXa with thrombin reveals that fIXa contains a Gln at position 192, similar to the thrombin E192Q mutant and fXa. In addition, previous studies have revealed that mutation of the homologous residue in fVIIa (Lys¹⁹²) to Gln enhances its reactivity with BPTI (29), and that mutation of Gln¹⁹² in fIXa altered its reactivity toward TFPI (40). Neither of these studies examined the potential effect of heparin on reactivity with these Kunitz inhibitors. These studies are intriguing and seem to implicate residue 192 in potential heparin responsiveness along with the 99-loop. The investigation of potential interplay between residue 192 and the 99-loop of fIXa in its response to heparin binding is beyond the scope of the present study, however, and must await future studies.

Acknowledgments—We thank Dr. Steven T. Olson for the generous gift of heparin-derived oligosaccharides (H6, H10, H14, and H18), Dr. Earl W. Davie for the factor IX cDNA clone, and Dr. Jolyon Jesty for the ThermoMax microplate reader control software, KINEMAX.

REFERENCES

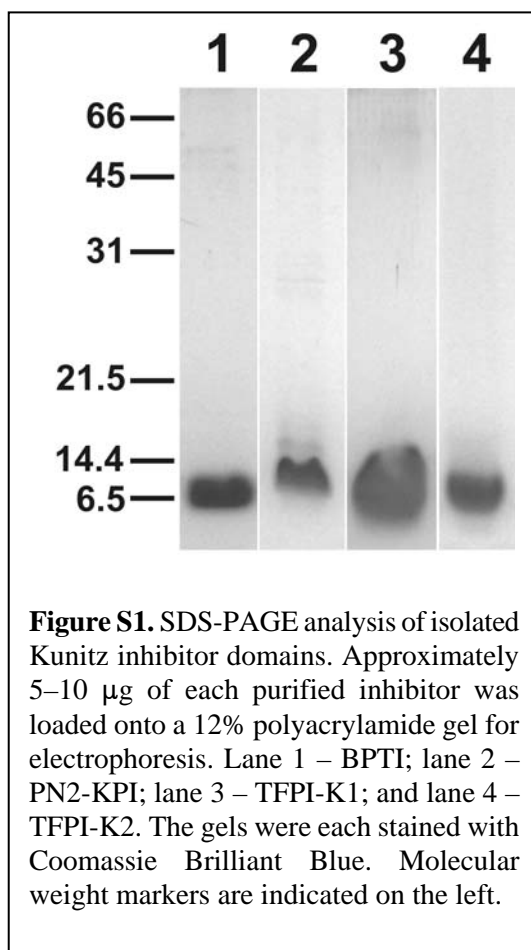
- Neuenschwander, P. (2006) in *Encyclopedia of Respiratory Medicine* (Laurant, G., and Shapiro, S., eds) pp. 509–514, Elsevier Ltd., Oxford, UK
- Jesty, J., and Nemerson, Y. (1995) in *Williams Hematology* (Beutler, E., Lichtman, M. A., Collar, B. S., and Kipps, T. J., eds) 5th Ed., pp. 1227–1238, McGraw-Hill, Inc., New York
- van Dieijen, G., Tans, G., Rosing, J., and Hemker, H. C. (1981) *J. Biol. Chem.* **256**, 3433–3442
- van Dieijen, G., van Rijn, J. L., Govers-Riemslog, J. W., Hemker, H. C., and Rosing, J. (1985) *Thromb. Haemostasis* **53**, 396–400
- Mertens, K., and Bertina, R. M. (1984) *Biochem. J.* **223**, 607–615
- Mertens, K., van Wijngaarden, A., and Bertina, R. M. (1985) *Thromb. Haemostasis* **54**, 654–660
- Rosenberg, J. S., McKenna, P. W., and Rosenberg, R. D. (1975) *J. Biol. Chem.* **250**, 8883–8888
- Kurachi, K., Fujikawa, K., Schmer, G., and Davie, E. W. (1976) *Biochemistry* **15**, 373–377
- DiScipio, R. G., Kurachi, K., and Davie, E. W. (1978) *J. Clin. Investig.* **60**, 1528–1538
- Villaneuva, G. B., and Danishefsky, I. (1977) *Biochem. Biophys. Res. Commun.* **74**, 803–809
- Villaneuva, G. B. (1984) *J. Biol. Chem.* **259**, 2531
- Olson, S. T., and Björk, I. (1992) *Adv. Exp. Med. Biol.* **313**, 155–165
- Olson, S. T., Björk, I., Sheffer, R., Craig, P. A., Shore, J. D., and Choay, J. (1992) *J. Biol. Chem.* **267**, 12528–12538
- Yang, L. K., Manithody, C., and Rezaie, A. R. (2002) *J. Biol. Chem.* **277**, 50756–50760
- Neuenschwander, P. F. (2004) *Biochemistry* **43**, 2978–2986
- Rezaie, A. R., Fiore, M. M., Neuenschwander, P. F., Esmon, C. T., and Morrissey, J. H. (1992) *Protein Expression Purif.* **3**, 453–460
- Neuenschwander, P. F., and Morrissey, J. H. (1994) *J. Biol. Chem.* **269**, 8007–8013
- Olson, S. T., Björk, I., and Shore, J. D. (1993) in *Methods in Enzymology* (Lorand, L., and Mann, K. G., eds) pp. 525–559, Academic Press, New York
- Lindahl, U., Thunberg, L., Bäckström, G., Riesenfeld, J., Nordling, K., and Björk, I. (1984) *J. Biol. Chem.* **259**, 12368–12376
- Olson, S. T. (1988) *J. Biol. Chem.* **263**, 1698–1708
- Anderer, F. A. (1965) *Z. Naturforsch. B* **20**, 462–472
- Anderer, F. A., and Hoernle, S. (1965) *Z. Naturforsch. B* **20**, 457–462
- Wagner, S. L., Siegel, R. S., Vedvick, T. S., Raschke, W. C., and Van Nostrand, W. E. (1992) *Biochem. Biophys. Res. Commun.* **186**, 1138–1145
- Wun, T. C., Kretzmer, K. K., Girard, T. J., Miletich, J. P., and Broze, G. J., Jr. (1988) *J. Biol. Chem.* **263**, 6001–6004
- Steinle, A., Li, P., Morris, D. L., Groh, V., Lanier, L. L., Strong, R. K., and Spies, T. (2001) *Immunogenetics* **53**, 279–287
- De Bernardez Clark, E., Hevehan, D., Szela, S., and Maachupalli-Reddy, J. (1998) *Biotechnol. Prog.* **14**, 47–54
- Kurachi, K., and Davie, E. W. (1982) *Proc. Natl. Acad. Sci. U. S. A.* **79**, 6461–6464
- Horton, R. M., Cai, Z., Ho, S. N., and Please, L. R. (1990) *BioTechniques* **8**, 528–535
- Neuenschwander, P. F., and Morrissey, J. H. (1995) *Biochemistry* **34**, 8701–8707
- Chase, T., Jr., and Shaw, E. (1967) *Biochem. Biophys. Res. Commun.* **29**, 508–514
- Mann, K. G., Williams, E. B., Krishnaswamy, S., Church, W., Giles, A., and Tracy, R. P. (1990) *Blood* **76**, 755–766
- Neuenschwander, P. F., McCollough, J., McCallum, C. D., and Johnson, A. E. (1997) *Thromb. Haemostasis* **78**, (suppl.) 428
- Morrison, J. F., and Walsh, C. T. (1988) *Adv. Enzymol.* **61**, 201–301
- Copeland, R. A. (1996) *Enzymes: A Practical Introduction to Structure, Mechanism, and Data Analysis*, pp. 225–261, VCH Publishers, Inc., New York
- Van Nostrand, W. E., Wagner, S. L., Farrow, J. S., and Cunningham, D. S. (1990) *J. Biol. Chem.* **265**, 9591–9594
- Petersen, L. C., Bjorn, S. E., Olsen, O. H., Nordfang, O., Norris, F., and Norris, K. (1996) *Eur. J. Biochem.* **235**, 310–316
- Wlodawer, A., Walter, J., Huber, R., and Sjolín, L. (1984) *J. Mol. Biol.* **180**, 301–329
- Hopfner, K. P., Lang, A., Karcher, A., Sichler, K., Kopetzki, E., Brandstetter, H., Huber, R., Bode, W., and Engh, R. A. (1999) *Struct. Fold Des.* **7**, 989–996
- Zhang, E., St. Charles, R., and Tulinsky, A. (1999) *J. Mol. Biol.* **285**, 2089–2104
- Hsu, Y. C., Hamaguchi, N., Chang, Y. J., and Lin, S. W. (2001) *Biochemistry* **40**, 11261–11269
- Piro, O., and Broze, G. J., Jr. (2004) *Circulation* **110**, 3567–3572
- Yuan, Q. P., Walke, E. N., and Sheehan, J. P. (2005) *Biochemistry* **44**, 3615–3625
- Sheehan, J. P., Kobbervig, C. E., and Kirkpatrick, H. M. (2003) *Biochemistry* **42**, 11316–11325
- Schmaier, A. H., Dahl, L. D., Hasan, A. A. K., Cines, D. B., Bauer, K. A., and Van Nostrand, W. E. (1995) *Biochemistry* **34**, 1171–1178
- Rezaie, A. R., He, X., and Esmon, C. T. (1998) *Biochemistry* **37**, 693–699

SUPPLEMENTAL DATA
 HEPARIN MODULATES THE 99-LOOP OF FACTOR IXA: EFFECTS ON REACTIVITY WITH ISOLATED
 KUNITZ-TYPE INHIBITOR DOMAINS
 Neuenschwander, P.F., Williamson, S.R., Nalian, A. and Baker-Deadmond, K.J.

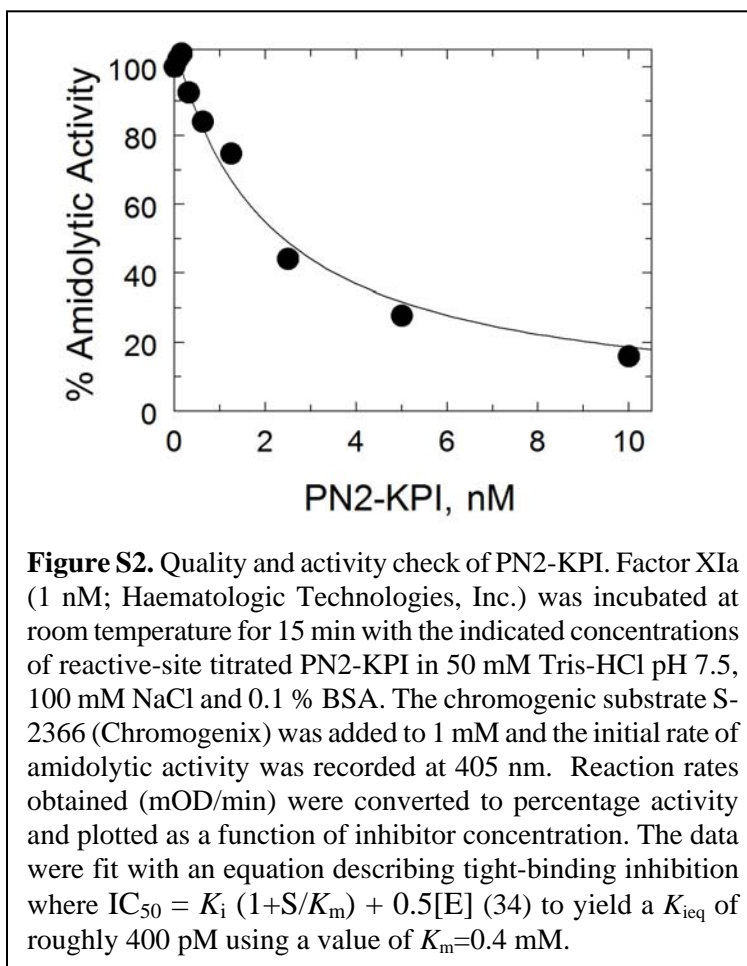
Table S1. Amino Acid Sequence Alignment of Kunitz-type inhibitor domains*

	1	10	20	30	40	50
BPTI	RPDFCLEPPY	TG PCK ARI	IIRYFYNAKAGLCQT	FVYGGCRAKR	NNFKSAEDCMRTC	GGGA
PN2-KPI	EVVREVCSEQAE	TG PCK RAMISR	WYFDVTEGKCAP	FFYGGCGGNR	NNFDTEEYCM	AVCGSA
TFPI-K1	MHSFCAFKAD	DG PCK AIMKR	FFNIFTRQCEE	FIYGGCEGNQ	NR	FESLEECKKMCTRD
TFPI-K2	KPDFCFLEED	PG ICR GYITR	YFYNNQTKQCE	FKYGGCLGNM	NNFETLEECK	KNICEDG
TFPI-K3	GPSWCLTPAD	RGL CR ANENR	FYNSVIGKCRP	FKYSGCGNE	NNFTSKQECL	RACKK

* Conserved amino acids with BPTI are shaded. Reactive site loops (thin boxes) and stabilizing loops (thick boxes) are held in close proximity by a disulfide bond between Cys₁₄ and Cys₃₈ (indicated). The P1 reactive site residues are in bold.



SUPPLEMENTAL DATA
HEPARIN MODULATES THE 99-LOOP OF FACTOR IXA: EFFECTS ON REACTIVITY WITH ISOLATED
KUNITZ-TYPE INHIBITOR DOMAINS
Neuenschwander, P.F., Williamson, S.R., Nalian, A. and Baker-Deadmond, K.J.



SUPPLEMENTAL DATA
 HEPARIN MODULATES THE 99-LOOP OF FACTOR IXA: EFFECTS ON REACTIVITY WITH ISOLATED
 KUNITZ-TYPE INHIBITOR DOMAINS
 Neuenschwander, P.F., Williamson, S.R., Nalian, A. and Baker-Deadmond, K.J.

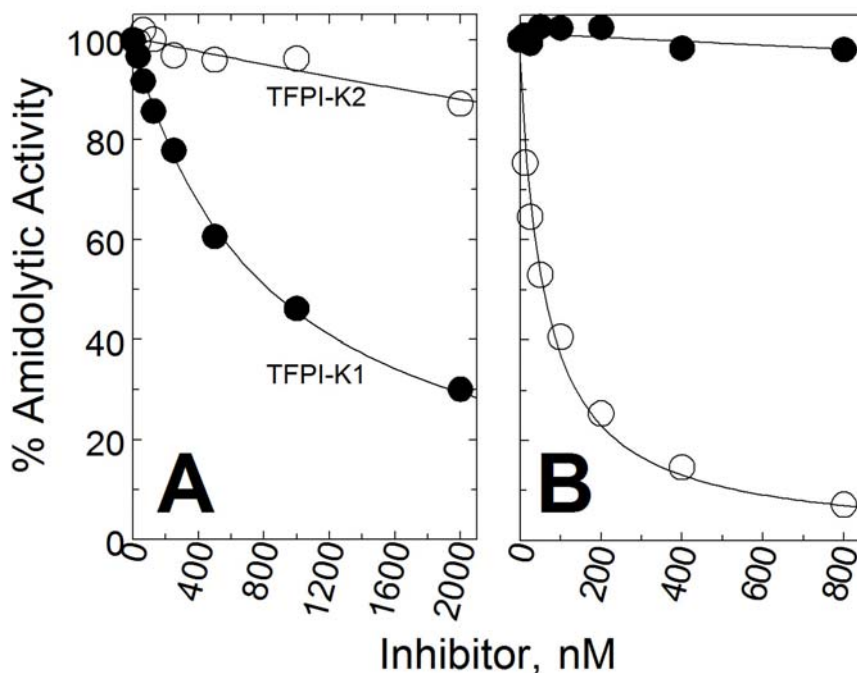


Figure S3. Quality and activity check of TFPI-K1 and TFPI-K2. *A.* Inhibition of the complex of factor VIIa and soluble tissue factor. The indicated concentrations of TFPI-K1 (●) or TFPI-K2 (○) were incubated with 5 nM factor VIIa (Haematologic Technologies, Inc.), 100 nM recombinant soluble tissue factor (16) and 5 mM Ca^{2+} in 20 mM Hepes-NaOH pH 7.4, 100 mM NaCl and 0.1% BSA for 15 minutes at room temperature as previously described (24). The chromogenic substrate Chromozym-tPA (Roche Diagnostics) was then added to 1 mM and the initial rate of amidolytic activity was monitored at 405 nm. Reaction rates obtained (mOD/min) were converted to percentage activity and plotted as a function of inhibitor concentration. Fits of the data with Equation 1 yielded K_{ieq} values of 400 nM for TFPI-K1 and $\sim 7 \mu\text{M}$ for TFPI-K2. *B.* Inhibition of factor Xa. The indicated concentrations of TFPI-K1 (●) or TFPI-K2 (○) were incubated with 5 nM factor Xa and 5 mM Ca^{2+} in 20 mM Hepes-NaOH pH 7.4, 100 mM NaCl and 0.1% BSA for 15 minutes at room temperature. The chromogenic substrate S-2222 (Chromogenix) was then added to 0.5 mM and the initial rate of amidolytic activity was monitored at 405 nm. Reaction rates (mOD/min) were converted to percentage activity and plotted as a function of inhibitor concentration. Fits of the data with Equation 1 yielded K_{ieq} values of $>1.5 \mu\text{M}$ for TFPI-K1 and 24 nM for TFPI-K2.